

# (1,1'-Ferrocenediyl)ferrocenyl(methyl)silane, Its Thermally Ring-Opened Polymer, and Oligomer Models

Keith H. Pannell,<sup>\*,†</sup> Vyacheslav V. Dementiev,<sup>†</sup> Hong Li,<sup>†</sup>  
Francisco Cervantes-Lee,<sup>†</sup> My T. Nguyen,<sup>‡</sup> and Art F. Diaz<sup>‡</sup>

Department of Chemistry, University of Texas at El Paso, El Paso, Texas 79968-0513, and  
IBM Almaden Research Center, 650 Harry Road, San Jose, California 95120

Received April 15, 1994<sup>®</sup>

The synthesis and spectroscopic and structural characterization of a ferrocenyl-substituted silyl-[1]-ferrocenophane, (1,1'-ferrocenediyl)ferrocenyl(methyl)silane, **1**, is reported. **1** crystallizes in space group  $P2_1/c$ , with  $a = 20.344(8)$  Å,  $b = 7.336(3)$  Å,  $c = 11.567(7)$  Å, and  $\beta = 90.51(4)^\circ$ . The dihedral angles between the two ferrocenophane cyclopentadienyl rings are  $21.3^\circ$ , and the ring centroid—Fe—ring centroid angle is  $164.3^\circ$ . Cyclic voltammetric analysis illustrates that both of the Fe centers, ferrocenyl and ferrocenophane, exhibit reversible redox behavior. This reversibility distinguishes the complex from other [1]-ferrocenophanes which exhibit irreversible oxidation under similar conditions. Thermal treatment of **1** results in facile polymerization to high molecular weight amorphous poly(ferrocenyleneferrocenyl(methyl)silane), **2**. The molecular weight of the polymer was considerably increased by performing the polymerization in solution as opposed to the melt,  $M_w = 210\,000$  vs  $45\,000$ . The electrochemical properties of the polymer indicate that neighboring Fe centers of the ferrocenylenesilane chain and pendant ferrocenyl groups interact, and four independent redox processes are observed. As a model for the ferrocenylenedialkylsilane polymers the synthesis and X-ray structure of 1,1'-bis(ferrocenyldimethylsilyl)ferrocene, **3**, is also reported. **3** crystallizes in space group  $P2_1/c$ , with  $a = 10.084(2)$  Å,  $b = 14.958(2)$  Å,  $c = 11.175(2)$  Å, and  $\beta = 114.98(1)^\circ$ . The ferrocenyl and ferrocenylene units are perpendicular to each other, and each of the Fe units exhibits an individual redox process upon cyclic voltammetric investigation. Molecular mechanics calculations reveal a range of structures with local energy minima for such oligomers, one of which is equivalent to the single-crystal X-ray structure obtained for **3**. The Fe—Fe distances in these conformers differ significantly, 6.1–6.9 Å, suggesting that high molecular weight polymers also possess a range of possible conformations and inter-Fe Coulombic interactions.

## Introduction

The synthesis and study of polymers and polymer precursors has developed into an extremely active aspect of organometallic chemistry since the resulting materials may be expected to possess many novel optical, electronic, and thermal properties.<sup>1</sup> We have previously noted that polysilanes with pendant ferrocenyl (Fc),  $(\eta^5\text{-C}_5\text{H}_5)\text{Fe}(\eta^5\text{-C}_5\text{H}_4)$ , groups were readily synthesized and exhibited reversible redox properties and modified photochemical depolymerization when compared to their non-Fc substituted analogs.<sup>2</sup> Foucher, Manners, and co-workers<sup>3</sup> and we<sup>4</sup> have reported that thermal ring opening of silicon bridged [1]-ferrocenophanes produced high molecular weight ferrocenylenesilane polymers, a reaction reminiscent of earlier

studies by Seyferth on phosphorus- and tin-bridged ferrocenophanes.<sup>5</sup> Tanaka has also studied related materials and noted that doped systems possess interesting conductance properties.<sup>6</sup> We have extended our initial study which dealt with alkyl substituents on silicon, Me, Et, *n*-Bu, and *n*-Hex, to systems that contain transition metal substituents and report the synthesis and characterization of one such member of the series, (1,1'-ferrocenediyl)ferrocenyl(methyl)silane, **1**, and the polymer it forms upon thermal ring opening, **2**. We also report the synthesis, structural characterization, and electrochemical properties of oligomers that model the ferrocenylenesilane polymers, i.e., 1,1'-bis(ferrocenyldimethylsilyl)ferrocene,  $(\eta^5\text{-FcSiMe}_2\text{C}_5\text{H}_4)\text{Fe}(\eta^5\text{-C}_5\text{H}_4\text{SiMe}_2\text{-}$

<sup>†</sup> University of Texas at El Paso.

<sup>‡</sup> IBM Almaden Research Center.

<sup>®</sup> Abstract published in *Advance ACS Abstracts*, August 1, 1994.

(1) (a) Zeldin, M.; Wynne, K. J.; Alcock, H. R. *Inorganic and Organometallic Polymers*; ACS Symposium Series 360; American Chemical Society: Washington, DC, 1988. (b) Mark, J. E.; Alcock, H. R.; West, R. *Inorganic Polymers*; Prentice Hall Polymer Science and Engineering Series; Englewood Cliffs, NJ, 1992.

(2) (a) Pannell, K. H.; Rozell, J. M.; Ziegler, J. M. *Macromolecules* **1988**, *21*, 278. (b) Pannell, K. H.; Rozell, J. M.; Vincenti, S. In *Silicon Based Polymer Science: A Comprehensive Resource*; Zeigler, J. M., Fearon, F. W. G. Eds.; Advances in Chemistry Series No. 224; American Chemical Society: Washington, DC, 1990; Chapter 20. (c) Diaz, A.; Seymour, M.; Pannell, K. H.; Rozell, J. M. *J. Electrochem. Soc.* **1990**, *137*, 503.

(3) (a) Foucher, D. A.; Tang, B.-Z.; Manners, I. *J. Am. Chem. Soc.* **1992**, *114*, 6246. (b) Tang, B.-Z.; Foucher, D. A.; Lough, A.; Coombs, N.; Sodhi, R.; Manners, I. *J. Chem. Soc., Chem. Commun.* **1993**, 523. (c) Foucher, D. A.; Ziembinski, R.; Tang, B.-Z.; Macdonald, P. M.; Massey, J.; Jaeger, C. R.; Vancso, G. J.; Manners, I. *Macromolecules* **1993**, *26*, 2878.

(4) (a) Dementiev, V. V.; Pannell, K. H. Presented at the XXVth Organosilicon Symposium, Los Angeles, April 1992; paper 34. (b) Dementiev, V. V.; Pannell, K. H.; Nguyen, M. T.; Diaz, A. F. Presented at the XXVth Organosilicon Symposium, Indianapolis, IN, 1993; paper 34. (c) Nguyen, M. T.; Diaz, A. F.; Dementiev, V. V.; Sharma, H.; Pannell, K. H. *SPIE Proc.* **1993**, *1910*, 230. (d) Nguyen, M. T.; Diaz, A. F.; Dementiev, V. V.; Pannell, K. H. *Chem. Mater.* **1993**, *5*, 1389.

(5) (a) Seyferth, D.; Withers, H. P. *Organometallics* **1982**, *1*, 1275. (b) Withers, H. P.; Seyferth, D.; Fellman, J. D.; Garrou, P. E.; Martin, S. *Organometallics* **1982**, *1*, 1283.

(6) Tanaka, M.; Hayashi, T. *Bull. Chem. Soc. Jpn.* **1993**, *66*, 334.

Table 1. Analytical and Spectral Data for 1-3<sup>a</sup>

	1		2		3	
	1,1'-FcMeSi[( $\eta^5$ -C <sub>5</sub> H <sub>4</sub> )Fe( $\eta^5$ -C <sub>5</sub> H <sub>4</sub> )]		[( $\eta^5$ -C <sub>5</sub> H <sub>4</sub> )Fe( $\eta^5$ -C <sub>5</sub> H <sub>4</sub> )-SiMeFc] <sub>n</sub> <sup>b</sup>		FcSiMe <sub>2</sub> [( $\eta^5$ -C <sub>5</sub> H <sub>4</sub> )Fe( $\eta^5$ -C <sub>5</sub> H <sub>4</sub> )]SiMe <sub>2</sub> Fc	
<sup>1</sup> H	0.64 (Me); 4.06, 4.18, 4.28, 4.47 (m, m, s, t, C <sub>5</sub> H <sub>4</sub> ); 4.14 (C <sub>5</sub> H <sub>5</sub> )		0.87 (Me); 4.01, 4.22 (bd m, (C <sub>5</sub> H <sub>4</sub> , C <sub>5</sub> H <sub>5</sub> ))		0.52 (Me); 4.03, 4.09, 4.21, 4.25 (C <sub>5</sub> H <sub>4</sub> , C <sub>5</sub> H <sub>5</sub> )	
<sup>13</sup> C	-4.19 (Me); 34.32 (C <sub>5</sub> H <sub>4</sub> , Si-C); 66.15 (C <sub>5</sub> H <sub>4</sub> , Si-C); 66.87 (C <sub>5</sub> H <sub>5</sub> ), 71.69, 74.16, 75.56, 76.14, 77.57, 77.89 (C <sub>5</sub> H <sub>4</sub> )		-3.23 (Me); 67.77 (C <sub>5</sub> H <sub>4</sub> , Si-C); 68.90 (C <sub>5</sub> H <sub>5</sub> ); 71.12 (C <sub>5</sub> H <sub>4</sub> , Si-C), 71.51; 71.77, 72.04, 73.99, 74.24 (C <sub>5</sub> H <sub>4</sub> )		-0.61 (Me); 68.6 (C <sub>5</sub> H <sub>5</sub> ), 71.1, 71.7, 73.5, 73.6 (C <sub>5</sub> H <sub>4</sub> )	
<sup>29</sup> Si	-10.32		-9.67		-6.41	
	UV/Vis		UV/Vis		UV/Vis	
	474 nm (333)		446 nm (279)		446 nm (42)	
Anal. calcd(found)	C, 61.20(60.91); H, 4.89(5.02)		C, 61.20(60.74); H, 4.89(5.14)		C, 60.92(60.81); H, 5.71(6.21)	

<sup>a</sup> NMR spectra recorded in C<sub>6</sub>D<sub>6</sub>; UV/vis in hexane (1, 3) and THF (2).

<sup>b</sup> Dr. I. Manners has notified us that his group has also obtained the low molecular weight form of 2 and included it in a tabulation of such polymers in a recent review; Manners, I. *Adv. Mater.* 1994, 6, 68.

Fc), 3, plus MMX calculations that illustrate the range of conformational isomers possible in such systems.

## Experimental Section

**Synthesis of 1,1'-FcMeSi[( $\eta^5$ -C<sub>5</sub>H<sub>4</sub>)Fe( $\eta^5$ -C<sub>5</sub>H<sub>4</sub>)]**, 1. A solution of 7.4 mL of TMEDA in 10 mL of hexane was placed in a three-necked, round-bottomed flask and treated with 30.9 mL of a 1.6 M hexane solution of *n*-butyllithium. After the mixture was stirred for 30 min a solution of 3.8 g (20.4 mmol) of Fe(C<sub>5</sub>H<sub>5</sub>)<sub>2</sub> in 170 mL of hexane was added dropwise over 30 min. After 6 h of stirring a yellow precipitate of the required dilithio salt formed, which was separated by decantation and washed twice with 50 mL of hexane. The resulting pale yellow solid was slurried by addition of 50 mL of hexane. To this mixture was added dropwise a 70 mL hexane solution of 4.95 g (16.6 mmol) of FcSiMeCl<sub>2</sub>. The solution was stirred for 15 h, and then the salts were removed by filtration and the filtrate was evaporated to dryness. Recrystallization of the red-orange residue at -30 °C (toluene:hexane = 1:5) yielded 5.8 g (14.0 mmol, 84%) of 1, mp 119–121 °C. The analytical and spectroscopic properties of the complex are recorded in Table 1.

**Thermal Polymerization of 1.** We performed the thermal ring-opening polymerization of 1 via two distinct routes: (a) sealing the solid complex 1 (1.0 g, 2.43 mmol) in a 10 mL Pyrex tube and heating to 125 °C for 1 h; (b), refluxing a toluene solution of 1 (1.3 g, 3.15 mmol in 15 mL) for 32 h. Workup involved dissolution of the polymer in 30 mL of toluene for the melt reaction, or dilution to 30 mL for the solution polymerization reaction, followed by precipitation by 200 mL of hexane. Yields were typically in the range 70–85%. Spectroscopic properties of the polymers obtained were identical and are recorded in Table 1. The molecular weights, monomodal distribution, were distinctly different for the

products of the two techniques used: technique a,  $M_w = 45\,000$ ,  $M_n = 20\,000$ ; technique b,  $M_w = 210\,000$ ,  $M_n = 175\,000$ .

**Synthesis of ( $\eta^5$ -FcSiMe<sub>2</sub>C<sub>5</sub>H<sub>4</sub>)Fe( $\eta^5$ -C<sub>5</sub>H<sub>4</sub>SiMe<sub>2</sub>Fc)**, 3. Into a 250 mL three-necked, round-bottomed flask was placed 3.2 g (8.6 mmole) of 1,1'-bis(chlorodimethylsilyl)ferrocene dissolved in 30 mL of THF. [1,1'-bis(chlorodimethylsilyl)ferrocene was synthesized from 1,1'-bis((dimethylamino)dimethylsilyl)ferrocene<sup>7a</sup> by literature procedures.<sup>7b</sup>]. To this solution was added 15 mmol of ferrocenyllithium prepared by literature procedures.<sup>8</sup> After the addition (2 h), the resulting mixture was stirred for 2 days. The solvent was removed under reduced pressure, and the residue was treated with 100 mL of hexane and stirred for 2 h. After filtration and removal of the solvent, the oily residue was heated to 50 °C (0.5 mm/Hg) to remove dibutylmercury and ferrocene. The resulting solid residue was dissolved in hexane (20 mL), and the solution was placed upon a silica gel chromatography column (25 × 2.0 cm) which was developed with hexane. An initial yellow band was collected with hexane and yielded ferrocene, a second orange/red band was collected to yield a small amount of an unidentified oil, while a third red band was collected and after removal of solvent, and recrystallization from hexane/benzene (1:1 by volume), produced 3 (2.0 g, 3.0 mmol, 40%) as a red, crystalline material, mp 148–9 °C.

A second synthetic pathway that involved the addition of ClSiMe<sub>2</sub>Fc to a THF slurry of dilithioferrocene, in the ratio 2:1, resulted in a 46% yield of 3 after workup as above.

**Electrochemistry.** Cyclic voltammetric analysis of the various complexes and polymers was performed in CH<sub>2</sub>Cl<sub>2</sub> solution (0.1 M tetraethylammonium tetrafluoroborate, 0.2 cm<sup>2</sup> Pt electrodes vs Ag/AgCl reference electrode) using equipment described previously.<sup>4</sup>

**Structural Determination. Complex 1.** Unit cell parameters were determined by least-squares fit of 23 reflections selected randomly in reciprocal space in the range 15–30° in 2 $\Theta$  giving a monoclinic cell, space group *P*2<sub>1</sub>/*c*, with  $a = 20.344(8)$  Å,  $b = 7.336(3)$  Å,  $c = 11.567(7)$  Å, and  $\beta = 90.51(4)^\circ$ .

Intensity data were collected in the  $\omega$ -scan mode with a scan range of 1.5° in  $\omega$  at variable speed of 3–20 deg/min. Background counts were taken with a stationary crystal and total background time to scan time ratio of 0.5. Three standard reflections were measured every 97 reflections and showed no significant decay. The data were corrected for Lorentz and polarization effects, but no absorption correction was made.

The structure was solved and refined using the SHELEXTL-PLUS software package on a Microvax II computer. Full-matrix least-squares refinement minimizing  $\sum w(F_o - F_c)^2$  was carried out with anisotropic thermal parameters for all non-hydrogen atoms. Hydrogen atoms were placed at calculated positions and were not refined. The weighting scheme has the form  $w^{-1} = \sigma^2(F) + gF^2$ , and the final *R* factors have the form  $R = \sum |F_o - F_c| / \sum F_o$  and  $R_w = [\sum w|F_o - F_c|^2 / \sum F_o^2]^{1/2}$  with the resulting values of 3.01% and 3.29%, respectively. Relevant parameters are given in Tables 2–4.

**Complex 3.** Unit cell parameters were determined by least-squares fit of 25 reflections selected randomly in reciprocal space in the range 15–30° in 2 $\Theta$  giving a monoclinic cell, space group *P*2<sub>1</sub>/*c*, with  $a = 10.084(2)$  Å,  $b = 14.958(2)$  Å,  $c = 11.175(2)$  Å, and  $\gamma = 114.9(1)^\circ$ .

Intensity data were collected in the manner noted above with a scan range of 1.2°, and a semi-empirical absorption correction with minimum/maximum transmission ratio of 0.433/0.547 was applied. The structure was solved and refined as noted above for 1 to give final *R* values of 4.62% and 9.28%. Relevant parameters are given in Tables 2–4.

(7) (a) Petterson, W. J.; McManus, S. P. *J. Poly. Chem. Poly. Chem. Ed.* 1974, 12, 837. (b) Kabanov, B. K.; Zaitsev, V. A.; Varfolomeeva, N. A.; Baukova, G. G.; Kozlova, T. N. *Zh. Obs. Khim.* 1972, 42, 956. (8) Seyferth, D.; Hofmann, H. P.; Burton, R.; Helling, J. F. *Inorg. Chem.* 1962, 1, 227.

Table 2. Structure Determination Summary

	complex	
	1	3
Crystal Data		
empirical Formula	C <sub>21</sub> H <sub>20</sub> Fe <sub>2</sub> Si	C <sub>34</sub> H <sub>38</sub> Fe <sub>3</sub> Si <sub>2</sub>
color; habit	red fragment	red irregular fragment
cryst size (mm)	0.4 × 0.2 × 0.4	0.28 × 0.28 × .40
cryst system	monoclinic	monoclinic
space group		
unit cell dimens	<i>P</i> 2 <sub>1</sub> / <i>c</i>	<i>P</i> 2 <sub>1</sub> / <i>c</i>
<i>a</i> (Å)	20.344(8)	10.084(2)
<i>b</i> (Å)	7.336(3)	14.958(2)
<i>c</i> (Å)	11.567(7)	11.175(2)
$\beta$ (deg)	90.51(4)	114.980(10)
<i>V</i> (Å <sup>3</sup> )	1726.2(14)	1527.9(5)
<i>Z</i>	4	2
fw	412.2	670.4
<i>D</i> (calc) (Mg/m <sup>3</sup> )	1.586	1.457
abs coeff (mm <sup>-1</sup> )	1.747	1.505
<i>F</i> (000)	848	696
Data Collection		
diffractometer used		Siemens R3m/V
radiation ( $\lambda$ , Å)		Mo K $\alpha$ (0.71 73)
<i>T</i> (K)		298
monochromator		highly oriented graphite cryst
2 $\theta$ range (deg)		3.5–45.0°
scan type		$\omega$
scan speed (deg/min)		variable; 3.00–20.00°/min in $\omega$
		1.20
scan range ( $\omega$ ) (deg)	1.50	
bkgd measurement		stationary cryst and stationary counter at beginning and end of scan, each for 25.0% of tot. scan time
		3 measd every 97 reflns
std reflns		
index ranges	-21 ≤ <i>h</i> ≤ 21, -7 ≤ <i>k</i> ≤ 0, 0 ≤ <i>l</i> ≤ 12	-1 ≤ <i>h</i> ≤ 10, -2 ≤ <i>k</i> ≤ 15, -11 ≤ <i>l</i> ≤ 10
reflncs colld	2628	2581
indpt reflncs	2267 ( <i>R</i> <sub>int</sub> = 25.73%)	1964 ( <i>R</i> <sub>int</sub> = 2.61%)
obsd reflncs	2004 ( <i>F</i> > 4.0 $\sigma$ ( <i>F</i> ))	1653 ( <i>F</i> > 3.0 $\sigma$ ( <i>F</i> ))
abs corr	N/A	semi-empirical
min/max transm		0.4326/0.5472
Solution and Refinement		
system used		Siemens SHELXTL PLUS (VMS)
solution		direct methods
refinement method		full-matrix least-squares
quantity minimized		$\Sigma w(F_o - F_c)^2$
absolute structure	N/A	$\chi = 0.0000(4)$ , where
extinction corr	N/A	$F^* = F[1 + 0.002\chi F^2/(\sin 2\theta)]^{-1/4}$
H atoms		riding model, fixed isotropic <i>U</i>
weighting scheme	$w^{-1} = \sigma^2(F) + 0.0000F^2$	$w^{-1} = \sigma^2(F) + 0.0703F^2$
no. of params refined	219	179
final <i>R</i> indices (obsd data) (%)	<i>R</i> = 3.01, <i>R</i> <sub>w</sub> = 3.29	<i>R</i> = 4.62, <i>R</i> <sub>w</sub> = 9.28
<i>R</i> indices (all data) (%)	<i>R</i> = 3.48, <i>R</i> <sub>w</sub> = 3.31	<i>R</i> = 5.58, <i>R</i> <sub>w</sub> = 13.39
goodness-of-fit	3.03	0.36
largest and mean $\Delta/\sigma$	0.200, 0.013	3.071, 0.835
data-to-param ratio	9.2:1	9.2:1
largest diff peak (e Å <sup>-3</sup> )	0.32	0.49
largest diff hole	-0.37	-0.42

The large thermal parameters for some of the atoms, particularly C(6), C(7), C(13), and C(14) and some anomalous bond distances, e.g. C(6)–C(7), are due to disorder in the Cp rings which could not be resolved except by constraining their geometry to a regular pentagon. An additional data set was collected on the same crystal at -100 °C in an attempt to resolve the disorder, but results similar to those at room temperature were obtained. It is of interest that the recently published structure of the related pentamer FcSiMe<sub>2</sub>{(η<sup>5</sup>-C<sub>5</sub>H<sub>4</sub>)Fe(η<sup>5</sup>-C<sub>5</sub>H<sub>4</sub>SiMe<sub>2</sub>)<sub>3</sub>Fc contained similar disorder that resulted in anomalous C–C bond lengths in the terminal cyclopentadienyl rings.<sup>9</sup>

**Molecular Mechanics Calculations.** These were performed using a standard software package, PCModel 4.0

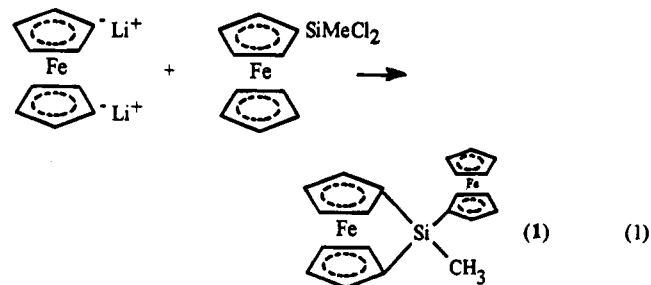
available from Serena Software, Bloomington, IN, on a Silicon Graphics Iris Indigo Xs-24 computer.

## Results and Discussion

**Monomer 1,1'-FcMeSi(η<sup>5</sup>-C<sub>5</sub>H<sub>4</sub>)Fe(η<sup>5</sup>-C<sub>5</sub>H<sub>4</sub>) (1) and Polymer 2.** Complex 1 was readily synthesized in high yield by the salt-elimination reaction illustrated in eq 1.

The spectroscopic data for 1 (Table 1) are in accord with the structure. Of note is the <sup>13</sup>C resonance for the ferrocenophane *ipso*-carbons at 34.3 ppm, and a <sup>29</sup>Si NMR resonance at -10.3 ppm, both values diagnostic of silyl-[1]-ferrocenophanes.<sup>3,4</sup>

We have performed a single-crystal X-ray analysis of 1, and the resulting structure is illustrated in Figure



1. Crystal data are presented in Table 2, atomic coordinates in Table 3, and selected bond lengths and angles in Table 4. The dihedral angle between the two ferrocenophane cyclopentadienyl rings is  $21.3^\circ$ , a value that may be compared to those reported for other [1]-ferrocenophanes, e.g.  $[(\eta^5\text{-C}_5\text{H}_3\text{R}')\text{Fe}(\eta^5\text{-C}_5\text{H}_4)]\text{ER}_2$  ( $\text{R}' = \text{H}$ ,  $\text{ER}_2 = \text{SiMe}_2$  ( $20.8^\circ$ ),<sup>3a</sup>  $\text{SiPh}_2$  ( $19.2^\circ$ ),<sup>10</sup>  $\text{GePh}_2$  ( $16.6^\circ$ ),<sup>11</sup>  $\text{PPh}$  ( $26.7^\circ$ ),<sup>10,12</sup>  $\text{R}' = \text{amine}$ ,  $\text{ER}_2 = \text{SiCl}_2$  ( $19.0^\circ$ )).<sup>13</sup> The corresponding Fe—Si distance in the ferrocenophane portion of the molecule is 2.71 Å; cf. those reported for the diphenyl- (2.63 Å) and dimethylsilyl- (2.69 Å) [1]-ferrocenophane analogs. The two ferrocene units in the molecule are somewhat aligned in a parallel fashion, and in both cases the two sets of cyclopentadienyl rings are almost completely eclipsed.

The electrochemical properties of ferrocenophanes have been well-studied.<sup>14</sup> Monoatom-bridged [1]-ferrocenophanes tend to exhibit nonreversible redox properties since oxidation causes the cyclopentadienyl—Fe distance to increase and a single atom bridge is unable to incorporate this size expansion.<sup>15</sup> However, oligosilyl-bridged [2]- and [3]-ferrocenophanes can accommodate this expansion and reversible redox properties ensue.<sup>16</sup> For 1 two reversible redox processes were observed, one for the ferrocenophane moiety,  $E_{\text{ox}} = 0.56$  V and  $E_{\text{red}} = 0.48$  V, and a second due to the pendant ferrocene group,  $E_{\text{ox}} = 0.68$  V and  $E_{\text{red}} = 0.48$  V. It appears that the addition of the pendant Fc unit permits a certain charge delocalization to occur upon oxidation of the ferrocenophane Fe atom thus facilitating a species that exhibits reversible oxidation on the cyclic voltammetric time scale. Attempts to produce stable oxidized complexes are in progress.

Complex 1 readily undergoes thermal ring-opening polymerization in the melt and in solution. The <sup>29</sup>Si NMR spectrum of the polymer exhibits a resonance at  $-9.70$  ppm, a value that does not show the "normal" high-field shift of 2–3 ppm when compared to the ferrocenophane monomers and polymers noted for the dimethyl, diethyl, di-*n*-butyl, and di-*n*-hexyl analogs.<sup>3c,4d</sup> The molecular weights of the polymers obtained from

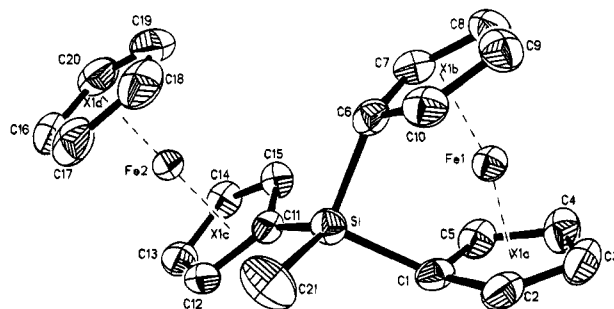


Figure 1. Structure of 1.

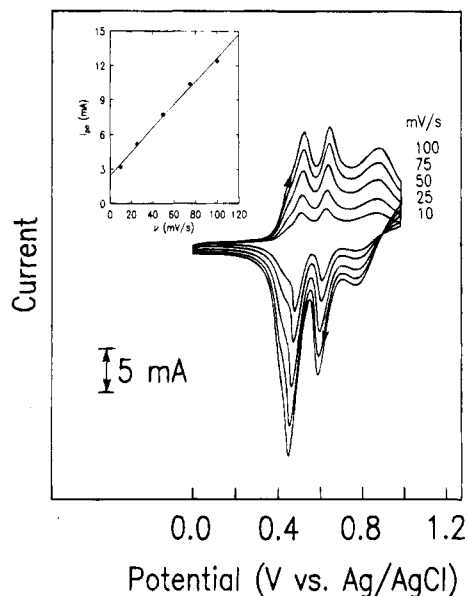


Figure 2. Cyclic voltammogram of 2, with inlay of  $I_{\text{pa}2}$  vs scan rate.

melt polymerization were in the range 40 000–50 000, ( $M_n = 19\ 000$ – $21\ 000$ ). However, when the polymerization was performed in solution, i.e., in toluene at temperatures between 90 and 110 °C, the polymers formed were of much higher molecular weights,  $M_w = 210\ 000$  ( $M_n = 175\ 000$ ). The polydispersity of the solution derived polymer was significantly less than the melt derived polymer, and an added advantage for the solution ring-opening polymerization is that the reaction may be followed by NMR spectroscopy by noting the disappearance of the <sup>29</sup>Si resonance at  $-10.3$  ppm and the appearance of the polymer resonance at  $-9.7$  ppm. Cyclic voltammetric analysis of the new polymer exhibits four reversible redox processes,  $E_{\text{ox}} = 0.49, 0.56, 0.68,$  and  $0.89$  V, Figure 2. These data indicate that, as with the dialkyl analogs, alternate ferrocenylene units are oxidized at different potentials due to the effect of neighboring units. Furthermore, alternant pendant ferrocenyl groups appear to be oxidized independently, subject to the Coulombic effect of both neighboring ferrocenylene and ferrocenyl groups. We suggest that the processes observed at  $E_{\text{ox}} = 0.49$  and  $0.89$  V are due to the ferrocenylene groups, and those at  $0.56$  and  $0.68$  V are due to the ferrocenyl groups. These assignments are in accord with previous observations of polymers containing ferrocenediyl and related redox active metal sites.<sup>3,4,9,17,18</sup> The peak heights are proportional to the

(10) Stoeckli-Evans, H.; Osborne, A. G.; Whiteley, R. H. *Helv. Chim. Acta* **1976**, *59*, 2402.

(11) Stoeckli-Evans, H.; Osborne, A. G.; Whiteley, R. H. *J. Organomet. Chem.* **1980**, *193*, 345.

(12) (a) Butler, I. R.; Cullen, W. R.; Einstein, F. W. B.; Rettig, S. J.; Willis, A. J. *Organometallics* **1983**, *2*, 128. (b) Butler, I. R.; Cullen, W. R.; Rettig, S. J.; *Organometallics* **1987**, *6*, 872.

(13) Butler, I. R.; Cullen, W. R.; Rettig, S. J. *Can. J. Chem.* **1987**, *65*, 1452.

(14) (a) Morrison, W. H.; Krogsrud, S.; Hendrickson, D. N. *Inorg. Chem.* **1973**, *12*, 1998. (b) Le Vanda, C.; Bechgaard, K.; Cowan, D. O. *J. Org. Chem.* **1976**, *41*, 2700.

(15) Churchill, M. R.; Landers, A. G.; Rheingold, A. L. *Inorg. Chem.* **1981**, *20*, 849.

(16) Dementiev, V. V.; Cervantes-Lee, F.; Párkányi, L.; Sharma, H.; Pannell, K. H.; Nguyen, M. T.; Diaz, A. F. *Organometallics* **1993**, *12*, 1983.

(17) Brandt, P. F.; Rauschfuss, T. B. *J. Am. Chem. Soc.* **1992**, *114*, 1926.

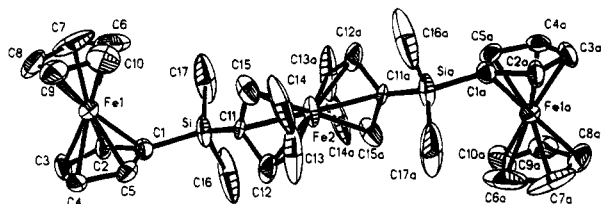
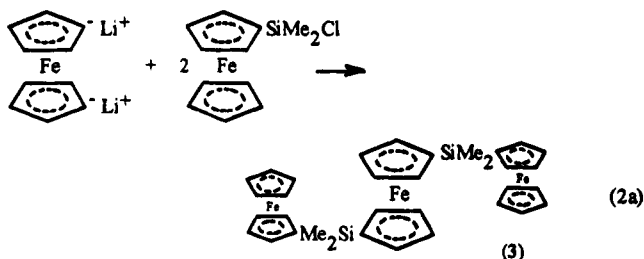


Figure 3. Structure of **3**.

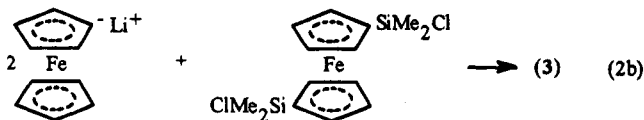
sweep rate suggesting the localization of the polymer at the electrode.<sup>4d</sup> Therefore, we studied the electrochemistry of the polymer as a thin film deposited on a platinum in a 0.1 M H<sub>2</sub>SO<sub>4</sub> solution, a condition where no dissolution of the polymer was observed. A clear distinction is observed between the solution electrochemistry and the thin film electrochemistry. The latter is typical of a poorly solvated insulating thin film that only becomes solvated, thus permitting conductivity, at a potential that causes physical disruption of the film (the "break-in" potential). In the present case this "break-in" potential exceeds the first oxidation potential of the solutions. A detailed study of the electrochemical and electrochromic aspects of poly(silane-ferrocenylene) thin films is reported elsewhere.<sup>19</sup>

Polymer **2** is not crystalline as determined by wide angle X-ray scattering and differential scanning calorimetry. This result may be compared with the dimethyl, diethyl, and di-*n*-butyl polymer analogs which exhibit significant ordering, whereas the di-*n*-hexyl polymer is completely amorphous and elastomeric. It is possible that different orientations of the Fc groups are responsible for the lack of crystallinity in the non-symmetrically-substituted silicon polymer.

**Oligomer ( $\eta^5$ -FcMe<sub>2</sub>SiC<sub>5</sub>H<sub>4</sub>)Fe( $\eta^5$ -C<sub>5</sub>H<sub>4</sub>SiMe<sub>2</sub>Fc) (**3**).** To obtain more information concerning the structure of the high molecular weight polymers, we have synthesized the first member of this series with two dimethylsilyl groups bridging three ferrocene units, i.e. ( $\eta^5$ -FcMe<sub>2</sub>SiC<sub>5</sub>H<sub>4</sub>)Fe( $\eta^5$ -C<sub>5</sub>H<sub>4</sub>SiMe<sub>2</sub>Fc), **3**, via the reaction between dilithioferrocene and (chlorodimethylsilyl)ferrocene, eq 2a.



An alternative route involved the reaction between lithioferrocene and 1,1'-bis(chlorodimethylsilyl)ferrocene, eq 2b.



(18) Collman, J. P.; McDevitt, J. T.; Leidner, C. R.; Yee, G. T.; Torrance, J. B.; Little, W. A. *J. Am. Chem. Soc.* **1987**, *109*, 4606.

(19) Nguyen, M. T.; Diaz, A. F.; Dementiev, V. V.; Pannell, K. H. *Chem. Mater.* **1994**, *6*, 952.

Table 3. Atomic Coordinates ( $\times 10^4$ ) and Equivalent Isotropic Displacement Coefficients ( $\text{\AA}^2 \times 10^3$ )

	x	y	z	<i>U</i> (eq) <sup>a</sup>
Compound 1				
Fe(1)	1083(1)	748(1)	3671(1)	31(1)
Fe(2)	3854(1)	745(1)	3609(1)	30(1)
Si	2277(1)	422(1)	4702(1)	33(1)
C(1)	1566(2)	2008(5)	4964(3)	34(1)
C(2)	945(2)	1324(5)	5359(3)	41(1)
C(3)	431(2)	2133(5)	4721(3)	48(1)
C(4)	708(2)	3347(5)	3927(3)	47(1)
C(5)	1395(2)	3290(5)	4075(3)	39(1)
C(6)	1879(2)	-826(5)	3455(3)	33(1)
C(7)	1707(2)	71(5)	2385(3)	38(1)
C(8)	1064(2)	-450(5)	2038(3)	42(1)
C(9)	826(2)	-1688(5)	2862(3)	41(1)
C(10)	1316(2)	-1934(5)	3717(3)	39(1)
C(11)	3015(2)	1741(5)	4332(3)	33(1)
C(12)	3576(2)	2048(5)	5065(3)	38(1)
C(13)	4037(2)	3107(5)	4480(3)	42(1)
C(14)	3788(2)	3492(5)	3365(3)	40(1)
C(15)	3165(2)	2672(5)	3279(3)	35(1)
C(16)	4703(2)	-711(6)	3535(3)	52(2)
C(17)	4207(2)	-1765(6)	4035(4)	57(2)
C(18)	3688(2)	-1911(5)	3214(4)	57(2)
C(19)	3869(2)	-957(6)	2224(4)	57(2)
C(20)	4492(2)	-226(6)	2418(3)	51(2)
C(21)	2437(2)	-1153(6)	5936(3)	60(2)
Compound 3				
Fe(1)	1378(1)	1089(1)	3681(1)	37(1)
Fe(2)	-5000	0	0	41(1)
Si	-2291(2)	1606(1)	1531(2)	47(1)
C(1)	-627(6)	1700(4)	3130(5)	36(2)
C(2)	542(7)	2350(4)	3504(6)	45(3)
C(3)	1545(8)	2182(5)	4851(7)	53(3)
C(4)	1034(7)	1428(5)	5310(6)	48(3)
C(5)	-285(7)	1144(4)	4271(6)	42(2)
C(6)	1375(17)	373(17)	2148(13)	173(11)
C(7)	2488(15)	972(9)	2537(13)	109(7)
C(8)	3411(8)	792(7)	3908(11)	83(5)
C(9)	2716(9)	-9(5)	4158(8)	60(4)
C(10)	1495(13)	-170(8)	3034(14)	96(7)
C(11)	-3118(6)	490(4)	1502(5)	25(2)
C(12)	-4208(7)	300(6)	1984(6)	55(3)
C(13)	-4569(12)	-615(10)	1791(11)	119(5)
C(14)	-3759(16)	-1009(6)	1204(12)	114(6)
C(15)	-2853(8)	-350(5)	1039(6)	59(3)
C(16)	-3736(11)	2485(5)	1510(2)	133(6)
C(17)	-1881(12)	1787(10)	97(8)	142(7)

<sup>a</sup> Equivalent isotropic *U* defined as one-third of the trace of the orthogonalized *U<sub>ij</sub>* tensor.

Table 4. Selected Bond Lengths ( $\text{\AA}$ ) and Angles (deg)

Compound 1			
Fe(1)-Si	2.708(2)	C(6)-Si-C(1)	95.6(2)
Si-C(6)	1.885(4)	C(11)-Si-C(21)	111.6(2)
Si-C(1)	1.884(4)	C(21)-Si-C(6)	110.89(2)
Si-C(11)	1.840(4)	C(1)-Si-C(11)	110.0(2)
Si-C(21)	1.863(4)	C(6)-Si-C(11)	115.1(2)
Compound 3			
Si-C(1)	1.870(5)	C(1)-Si-C(11)	107.4(2)
Si-C(16)	1.883(10)	C(11)-Si-C(16)	108.1(4)
Si-C(11)	1.861(6)	C(11)-Si-C(17)	112.4(5)
Si-C(17)	1.835(12)	C(1)-Si-C(16)	108.1(4)
Fe(1)-C(1)	2.062(6)	C(17)-Si-C(16)	108.3(6)
Fe(2)-C(11)	2.065(4)	C(1)-Si-C(17)	112.4(4)

In terms of yield, neither route is preferable. However, the formation of dilithioferrocene, eq 2a, does not require the use of (chloromercurio)ferrocene (the preferred precursor to quantitative formation of monolithioferrocene) and hence disposal of mercury compounds is not a consideration. The spectroscopic properties of **3** (Table 1) are unexceptional. A cyclic voltammetric electrochemical examination of **3** exhibited

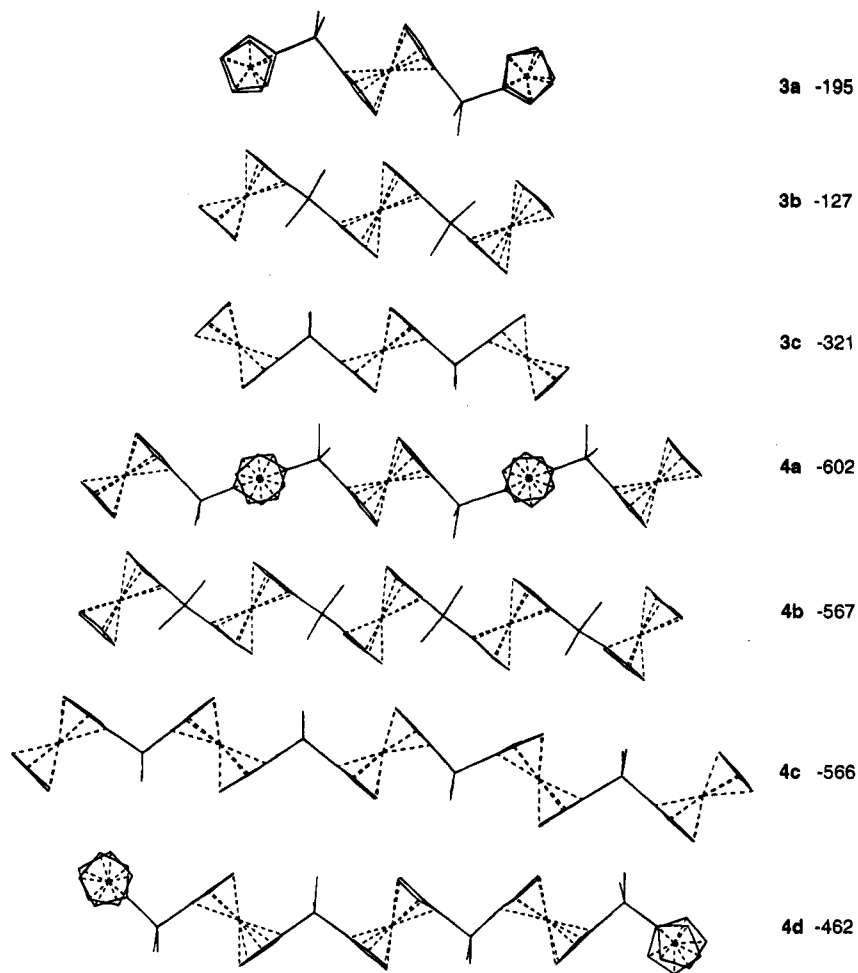


**Figure 4.** MMX calculated structures and energies (kcal/mol) of **3** and **4**.

three redox processes suggesting that each of the three ferrocene units exhibits a unique redox couple,  $E_{\text{ox}} = 0.57, 0.68, \text{ and } 0.85 \text{ V}$  and  $E_{\text{red}} = 0.53, 0.62, \text{ and } 0.79 \text{ V}$ . This pattern differs from that observed for the dialkylsilane ferrocenylene polymers where only two redox processes were noted reflecting oxidation of alternate Fe centers, the second at higher potential due to the Coulombic effect of the neighboring ferrocenium species formed by the initial oxidation. The first oxidation of **3** appears as a shoulder on the second oxidation feature in the cyclic voltammogram, and the difference between this and the polymers may reflect some conformational differences between the two systems affecting the Fe—Fe distances. The approach of the first and third ferrocene units in **3** may be closer than in the polymer, or a number of various conformations of the polymer could average out the oxidations of the Fe centers.

To provide more information on the structural aspects of the polymer systems we have determined the structure of **3** via single-crystal X-ray diffraction (Figure 3). The crystal data are presented in Table 2, atomic coordinates in Table 3, and selected bond lengths and angles in Table 4. It is immediately clear that the three ferrocene units form a chain in which each is perpendicular to its neighbor and not, as might have been the case, arranged in a stepwise formation. Each of the individual Fe—C and C—Si bond lengths and angles are in the expected range. The structure is similar to that of the recently published pentamer, containing three ferrocenylene units between two ferrocenyl groups, i.e.,  $\text{FcSiMe}_2\{(\eta^5\text{-C}_5\text{H}_4)\text{Fe}(\eta^5\text{-C}_5\text{H}_4\text{SiMe}_2)\}_3\text{Fc}$ , in which the

middle ferrocenediyl groups appear as *trans* zigzag series between perpendicularly oriented terminal Fc groups.<sup>9</sup> To evaluate the generality of this structure as a model for the oligomeric and polymeric materials we have performed some MMX calculations on the molecule and noted the variation of energy as a function of the relative orientation of the two Fc units about the central ferrocenylene group. The single-crystal structure determined for **3** is indeed a low-energy structure (−195 kcal/mol), calculated using the MMX software package, **3a**, Figure 4. However, other local energy minima exist in which the two Fc units are each rotated about the Si—ferrocenediyl bond away from the central  $(\eta^5\text{-C}_5\text{H}_4)\text{-Fe}(\eta^5\text{-C}_5\text{H}_4)$  unit in an opposite manner, **3b** (−127 kcal/mol). A structure with a ladderlike parallel sequence, **3c**, is another low-energy structure (−321 kcal/mol); i.e., there are several local minimum energy structures available for this simple three ferrocene unit complex. The actual crystal structure obtained by X-ray analysis consequently is not necessarily representative of the polymer, and indeed the five ferrocene unit recently described further underlines this fact.<sup>9</sup> The Fe—Fe distances in the three calculated conformers **3a–c** differ significantly: **3a**, 6.3 Å; **3b**, 6.1 Å; **3c**, 6.9 Å. Thus the ideas noted above concerning the various conformers and the observations of multiple redox processes in oligomers, but not in the polymers, seem plausible. The polymers exhibit only a partial crystalline nature; hence, it is probable that an array of structural conformers exists, with a range of Fe—Fe distances that will affect the strength of the Coulombic interactions that give rise

to multiple redox processes. The presence of two different groups on the Si atoms in the polymer and oligomer backbone will further increase the number of configurational isomers present and reduce the regularity of the systems. MMX calculations on the five ferrocene system also indicated a range of potential low-energy structures, and some of them are outlined in Figure 4b. Structures **4a–c** are equivalent to **3a–c**, and **4d** is similar to the structure reported for **4**.<sup>9</sup> As with **3**, a range of Fe–Fe distances was obtained, 6.0–6.9 Å.

**Acknowledgment.** This research has been supported by the NSF via Grant No. RII-88-02973 and the R. A. Welch Foundation, Houston, TX.

**Supplementary Material Available:** Tables of complete bond lengths and bond angles, anisotropic thermal parameters, and H atom positional and thermal parameters for **1** and **3** (8 pages). Ordering information is given on any current masthead page.

OM940288Z